Int. J. Electrochem. Sci., 11 **(2016)** 9326 – 9339, doi: 10.20964/2016.11.63

International Journal of ELECTROCHEMICAL SCIENCE
www.electrochemsci.org

In Vitro Bioactivity, Degradation Property and Cell Viability of the CaP/Chitosan/Graphene Coating on Magnesium Alloy in m-SBF

Jie Zhang[1,2*], *Fangfang Zhu*[1] , *Yu Zhang*[1], *Ming Hu*[1], *Yanxia Chi*[1],*Xiangyu Zhang*[1], *Xiaoling Guo*[1]

[1] Pharmaceutical Research Institute in Heilongjiang Province, Jiamusi university, Jiamusi 154007, China
[2] Department of neuro intern, First Affiliated Hospital of Harbin Medical University, Harbin 150001, China
[*]E-mail: zjie612@163.com

Received: 8 August 2016 / *Accepted:* 15 September 2016 / *Published:* 10 October 2016

CaP/chitosan/graphene coating on Mg alloy was obtained by electrophoretic deposition (EPD) and transformation in a phosphate buffer solution (PBS). The microstructures and compositions of the composite coatings were studied by scanning electron microscope (SEM), Fourier–transformed infrared spectroscopy (FTIR), X-ray diffraction (XRD) and Raman spectroscopy. The element concentration was investigated by inductively coupled plasma optical emission spectrometer (ICP-OES) test. The degradation behavior of Mg based CaP/chitosan/graphene in m-SBF was researched by soaking experiment and electrochemical performance test. The cytotoxicity of the prepared material to SaOS-2 cells was determined by CCK assay. The results indicated that addition of graphene had a positive effect on improving the bioactivity and cell viability of the CaP/chitosan coating. CaP/chitosan/graphene coating could protect the Mg alloy from corroding in m-SBF.

Keywords: Graphene, Mg alloy, Bioactivity, Hydroxyapatite, Bone-like apatite

1. INTRODUCTION

Magnesium and its alloys were excellent implants due to their biodegradability and biocompatibility. Further, the Young's modulus of magnesium and its alloys (45 GPa) are closer to natural bone (10-15 GPa), which may minimize the stress shielding and avoid the second surgery [1,2]. The degradation products of magnesium and its alloys are non-toxic and the redundant Mg^{2+} can be harmlessly excreted in the urine [3]. As the fourth most abundant cation in the human body, magnesium is an essential element to human metabolism and can promote bone cell attachment and tissue growth [4]. However, magnesium and its alloys can be corroded in the human body environment

too fast to keep the mechanical integrity before sufficient recovery. Researchers have demonstrated that the bioactive ceramic coating on magnesium and its alloys might be an effective way to decrease their corrosion rate [5-7]. Hydroxyapatite ($Ca_{10}(PO_4)_6(OH)_2$, HA), having the similar chemical and crystallographic structures of natural bone, has been extensively used for bone substitutes and other biomedical implants due to its bioactivity, biocompatibility and osteoconductive properties [8]. Due to the brittleness of pure HA, the addition of CNTs as a secondary constituent into bioactive film has been extensively explored to improve the overall mechanical properties of composites, such as toughness, elastic modulus, hardness and bending strength [9]. However, the biocompatibility of CNTs is still contradictory, though its cytotoxic effect in some cases result from impurities or aggregation and is not itself [9]. In contrast to CNTs, graphene exhibits little cytotoxicity due to its single layer structure is very simple and it can be synthesized in a relative pure form. Some researches have revealed that graphene is not toxic for mesenchymal stromal cells (MSCs) and human osteoblasts, and it can stimulate their adhesion and proliferation and facilitate the formation of bone-like apatite [10,11]. On the other hand, graphene exhibits more significant toughing effect on brittle materials than do CNTs [11,12]. Chitosan is a partially deacetylated polymer of N-acetyl glucosamine and one of the most promising biopolymers for tissue engineering, and it has possible orthopedic applications due to its good biocompatibility, intrinsic antibacterial activity and the ability to bind to growth factors[13,14]. Bone consists of an organic collagen matrix and inorganic hydroxyapatite[15]. As we know, the perfect bone substitutes should have higher mechanical property, good biocompatibility, bioactivity and a suitable biodegradation rate. From the structure of natural bone, it was proposed in this work to develop a novel MAO-AZ91D based CaP/chitosan/graphene as bone tissue material. Based on the previous studies[16-18], the bioactivity, corrosion properties and cell toxicity of Mg based CaP/chitosan/graphene were studied.

2. MATERIALS AND METHODS

2.1 Pretreatment of Mg alloy[18]

AZ91D Mg alloy (Dongqi Magnesium Alloy Products Co., Ltd., China) as the matrix material was cut into the quadrate samples with size of 1 cm×1 cm×0.5 cm. The quadrate samples welded with wires were packaged into the epoxy resin with one exposed surface of 1cm^2. The obtained specimens were burnished by the sandpaper and were ultrasonically washed.

A strong alkaline solution was used as the electrolyte of the MAO process. The treated Mg alloy sample was the anode and a stainless steel vessel with the electrolyte was the cathode. The MAO course was operated at a stable current of 0.1 A/cm^2 for 10-15s. The obtained oxidation specimens were ultrasonically washed and dried under room temperature.

2.2 preparation of Mg based CaP /chitosan/graphene

Just as the preliminary work, nano-hydroxyapatite (*n*HA) particles for EPD was synthesized by the chemical precipitation technology [19]. CS (a deacetylation degree of about 85%, M_w =200,000)

was from Sigma-Aldrich Trading Co, Ltd., China. 0.25 g CS, 1.0 g *n*HA particles were added into 200 ml of an acetic acid aqueous solution in the condition of agitation, respectively. The other solution was obtained by putting 1.5 g *n*HA particles into 300 ml absolute ethanol. At last, 0.01g of graphene was added into the mixture system of two solutions. The obtained mixture was sonicated for 1-2 h and aged for 24-30 h. Mg alloy was used as the cathode and the titanium alloy coated iridium tantalum was used as as the anode in the EPD. The EPD process was conducted under a voltage of 40 V for 20 min. After EPD, Mg alloy with the CaP/chitosan/graphene coating was immersed in a conical bottle with PBS at 37 °C for 5 d. The PBS was replaced every day. The obtained specimen was washed with the distilled water and dried under the room temperature.

2.3 Soaking into the m-SBF

After soaking into the PBS, Mg based CaP/chitosan/graphene was placed into a conical flask with 250 ml of the m-SBF at 37°C for different time intervals, respectively [20,21]. The ratio of the m-SBF volume (ml) to the specimen surface area (cm^2) was 250: 1. At the each time point, the specimens were took out from the m-SBF, washed with the ionized water, and dried under the room temperature.

2.4 Specimens characterization

After soaking into the m-SBF for the different periods, the surface morphologies of the composite coatings were observed by a SEM (S4800HSD, Japan). The composite coatings' compositions were studied by the XRD (Rigaku D/max-γB, Japan), FTIR (AVATAR360, Nicolet Instruments, USA) and Raman spectrometer (DXR, Thermo scientific, America). The pH value and elements concentration in the m-SBF were measured with a pH meter (PHS-3C, Shanghai Leici, China) and an ICP-OES (5300DV, Perkin Elmer, America), respectively.

Electrochemical impedance spectroscopy (EIS) test was conducted in m-SBF by using a Model CHI750D potentiostat (Chenhua Co., Ltd, Shanghai, China). Spectra of electrochemical impedance were recorded with the scan frequency ranging from 100 kHz to 10 mHz and a perturbation amplitude of 5 mV. The obtained Nyquist plots were fitted by the software Zsip Win 3.0. The scan rate of Tafel curve test was 5 mV/s, polarization time was 2 s.

2.5 Cell viability test of the extracts from the immersion test

The cytotoxicity of Mg based CaP/chitosan/graphene sample to SaOS-2 cells was determined by CCK assay. The soaking extracts collected from the soaking test were used to cultivate cells in this test. First day, 1×10^4 cells/100μl SaOS-2 human osteoblasts were cultivated in 1640 medium (Sigma company) on the 96-well plates (Corning company) at 37 ℃ in an atmosphere of 5% CO_2 and 95% air for one day. The medium in every well was substituted by 100 μl m-SBF extracts and 15% (v/v) fetal bovine serum (FBS, Hyclone, America) on the second day. The medium in every well was replaced with 90 μl m-SBF extracts and 10 μl CCK8 (Japanese), and incubated 37 ℃ in an atmosphere of 5%

CO_2 and 95% air for 1-4 h on the third day. The absorbance was recorded by enzyme standard instrument at 450 nm to determine the cell viability.

3. RESULTS AND DISCUSSION

3.1 In vitro bioactivity of Mg based CaP/chitosan/graphene in m-SBF

Fig.1 shows XRD pattern of the CaP/chitosan/graphene coating immersed in the m-SBF for different periods. It was clearly seen from Fig.1 that the diffraction peaks at 2θ=25.9, 31.8, 32.2, 32.9, 39.8, 46.7, 49.5, 53.1 were attributed to the major peaks of hydroxyapatite (HA, $Ca_{10}((PO_4)_6(OH)_2)$, and the characteristic peaks of bone-like apatite (HCA, $Ca_{10}(PO_4)_3(CO_3)_3(OH)_2$) were present at 2θ=25.7, 29.3, 32.2, 33.4. In Fig.1(a), the main ingredients in the CaP/chitosan/graphene coating were DCPD, HA and HCA before soaking into m-SBF, and DCPD would change into HA and HCA after soaking into m-SBF as shown in the previous study [16]. Compared to the sample before soaking into m-SBF (Fig.1(a)), the peaks of HA and HCA strengthened after the CaP/chitosan/graphene coating was soaked in the m-SBF in Fig.1(b-i), which showed that the amounts of HA and HCA increased. It was found from Fig.1(b-i) that the peak strengths and widths of HA and HCA changed little with the increase of the immersion time in m-SBF, suggesting that the changes of crystalline and the growing amount of HA and HCA in the m-SBF at the adjacent interval were difficult to be tested within the sensitivity limit of XRD.

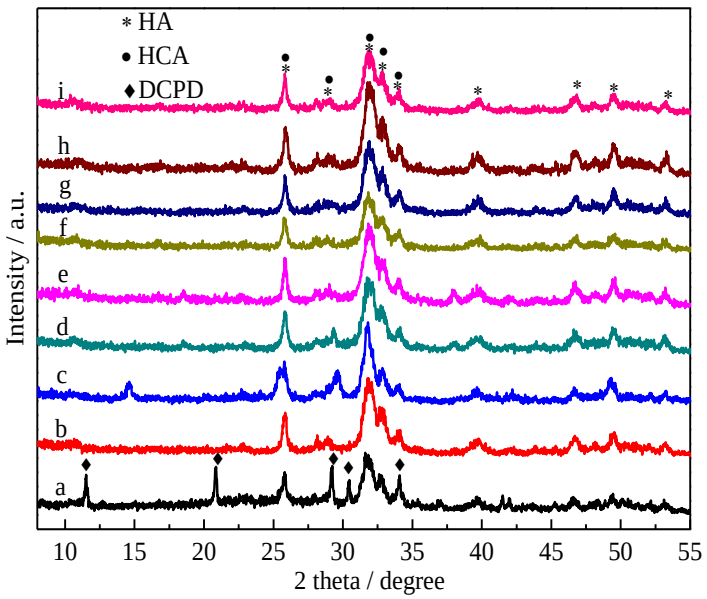

Figure 1. XRD patterns of the CaP/chitosan/graphene coating soaked in the m-SBF for different periods (a) 0 week (b) 1 week (c) 2 weeks (d) 3 weeks (e) 4 weeks (f) 6 weeks (g) 8 weeks (h) 10 weeks (i) 12 weeks

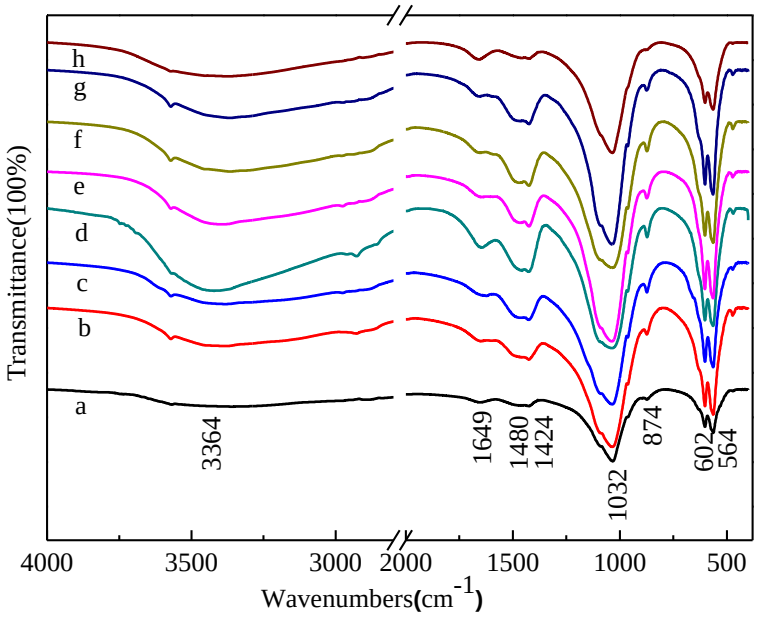

Figure 2. FT-IR spectra of the CaP/chitosan/graphene coating soaked in the m-SBF for different periods (a) 0 week (b) 1 week (c) 2 weeks (d) 4 weeks (e) 6 weeks (f) 8 weeks (g) 10 weeks (h) 12 weeks

Fig.2 shows FT-IR spectra of the CaP/chitosan/graphene coating soaked in the m-SBF for different periods. A strong absorption at 1032 cm^{-1} was attributed to ν_3 asymmetrical stretching of P-O. The peaks at 564 cm^{-1} and 602 cm^{-1} which referred to ν_4 P-O bending in PO_4^{3-} were observed. The bands at 3364 cm^{-1} and 1649 cm^{-1} corresponded to the hydroxyl group in the FT-IR spectra [22]. The peaks at 1424-1480 cm^{-1} and 874 cm^{-1} were assigned to the stretching vibrations of CO_3^{2-} [23]. It could be seen from Fig.2 that the absorption peaks of PO_4^{3-} and CO_3^{2-} obviously increased after the CaP/chitosan/graphene coating were immersed in m-SBF from 0 week to 10 weeks, which suggested that HA or HCA grew on the coating with the increase of soaking time. It could be concluded that the incorporation of graphene into the CaP/chitosan coating facilitated the formation of phosphate on the coating [11]. Up to 12 weeks, the peak strengths of PO_4^{3-} and CO_3^{2-} decreased, indicating the deposition process of phosphate relatively became weak at this phase.

Fig.3 is Raman spectra of the CaP/chitosan/graphene coating soaked in the m-SBF for different periods. The G-band at ~1597 cm^{-1} and the D-band at 1347 cm^{-1} were attributed to the Raman spectra of graphene, which showed that the graphene existed in the CaP/chitosan coating [24]. One sharp peak at 961 cm^{-1} was associated with the P-O stretching vibration of ν_1 (PO_4) mode, which was assigned to a typical feature of crystalline HA. A peak at 1085 cm^{-1} was attributed to ν_3 (PO_4) [25]. It could be seen from Fig.3 that a peak around 961 cm^{-1} became sharp with the soaking time increasing from 0 week to 4 weeks, indicating that the amount of HA increased [26]. When the immersion time changed from 4 weeks to 12 weeks, the strengths of HA peak dramatically decreased, indicating the deposition of HA changed into the dissolution process at this phase. It could be concluded from Fig.2 and Fig.3 that the graphene was more beneficial for the growth of bone-like apatite in m-SBF and its deposition process gradually strengthened as the immersion time from 0 week to 10 weeks. Moreover, a peak at 1083 cm^{-1}

weakened after the coating was immersed in m-SBF, which could be attributed to DCPD turning into HA and HCA as stated in previous study[16].

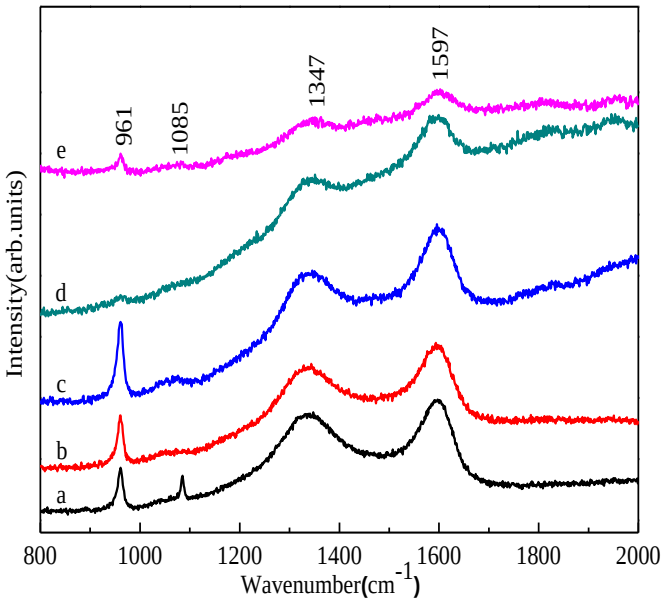

Figure 3. Raman spectra of the CaP/chitosan/graphene coating soaked in the m-SBF for different periods (a) 0 week (b) 1 week (c) 4 weeks (d) 10 weeks (e) 12 weeks

Fig.4 shows the changes of different element concentrations and pH value in m-SBF with the soaking time for Mg based CaP/chitosan/graphene. It could be seen from Fig.4(a)(b) that the element concentrations of Ca and P obviously decreased from 0 week to 4 weeks, which indicated that the deposition process of HA and HCA occurred. The element concentrations of Ca and P showed a slow decreasing trend during immersion phase from 6 weeks to 12 weeks, which suggested that the total deposition of phosphate became slow because the precipitation of HCA was accompanied by the dissolution of HA.

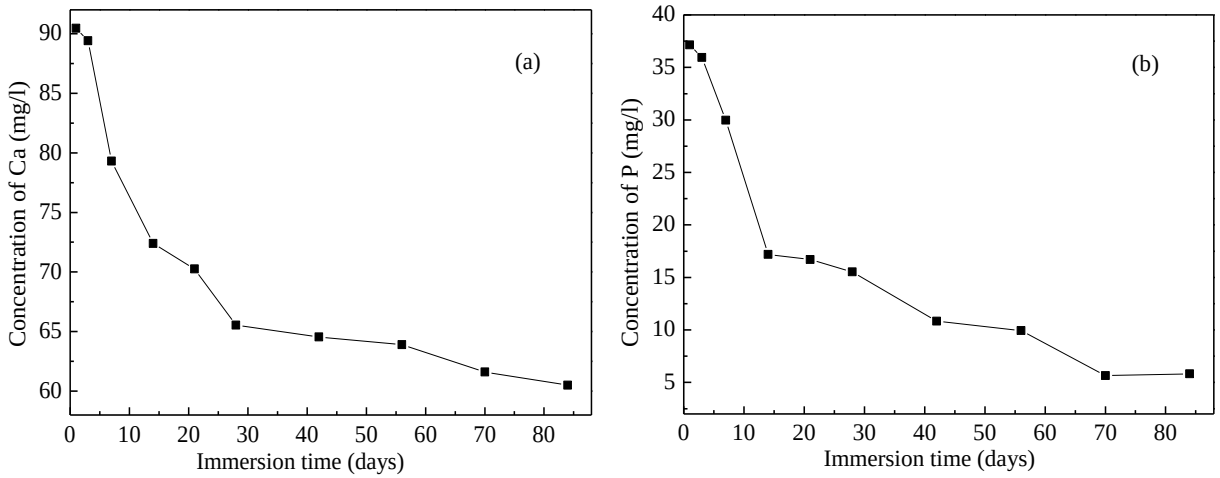

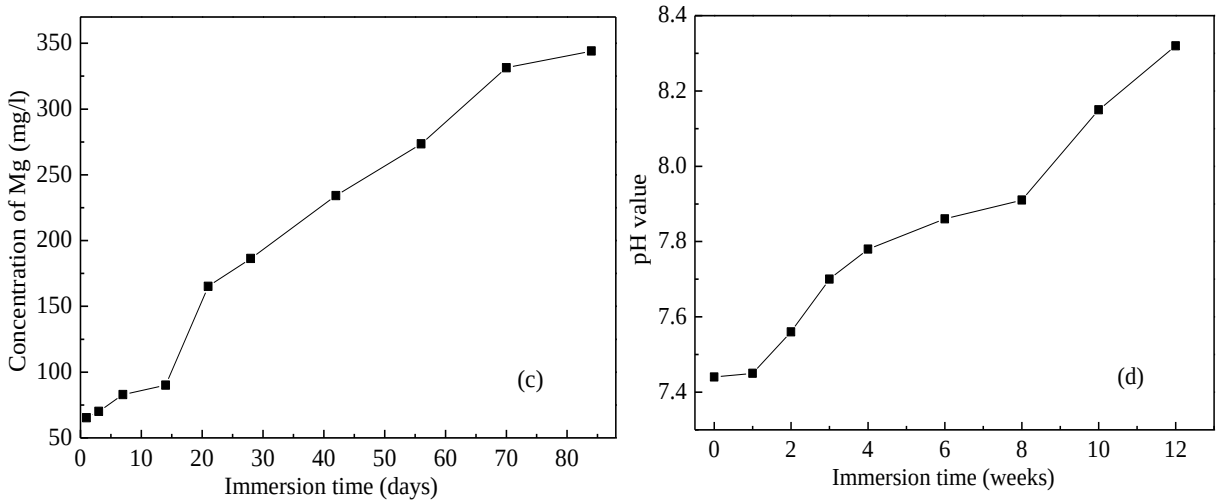

Figure 4. The changes of different elements concentrations and pH value in the m-SBF with the soaking time for Mg based CaP/chitosan/graphene (a) Ca (b) P (c) Mg (d) pH values

These were in agreement with the results of FIIR in Fig.2 and Raman in Fig.3. From Fig.4(c)(d), the Mg element concentration and pH value constantly increased at all immersion phase, suggesting the CaP/chitosan/graphene coating could not prevent the corrosion of Mg alloy in m-SBF as shown previous study [18].

Fig.5 shows SEM of the CaP/chitosan/graphene coating immersed in the m-SBF for different periods. It could be seen from Fig.5(a) that the morphology of the obtained coating showed the clubbed-like structure, which was attributed to the existence of HA and DCPD in the coating before soaking into m-SBF as shown in previous study [16]. Incidentally, the micropores in the coating resulted from the hydrogen release in EPD. Because the DCPD could turn into HA and HCA and a part of HA would dissolve when the obtained coating was immersed into m-SBF, a few graphene was exposed in the CaP/chitosan coating in Fig.5(b)(c).

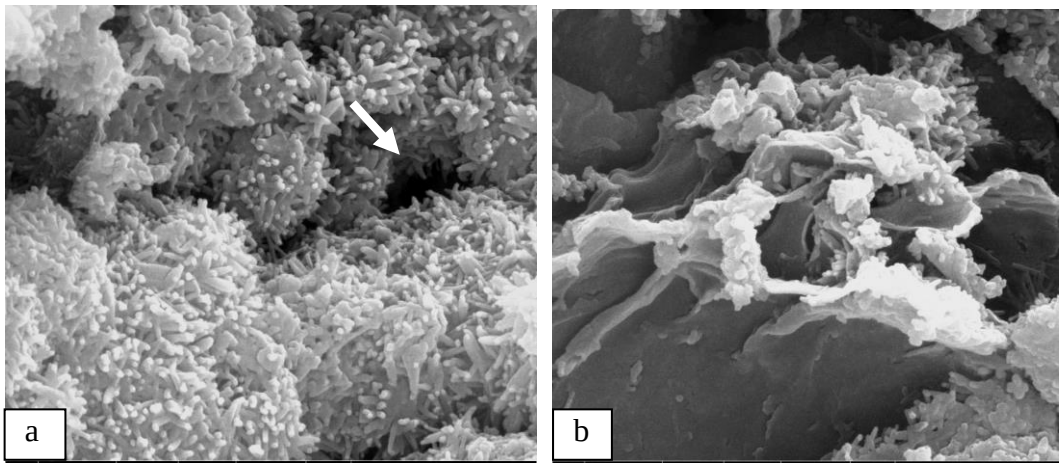

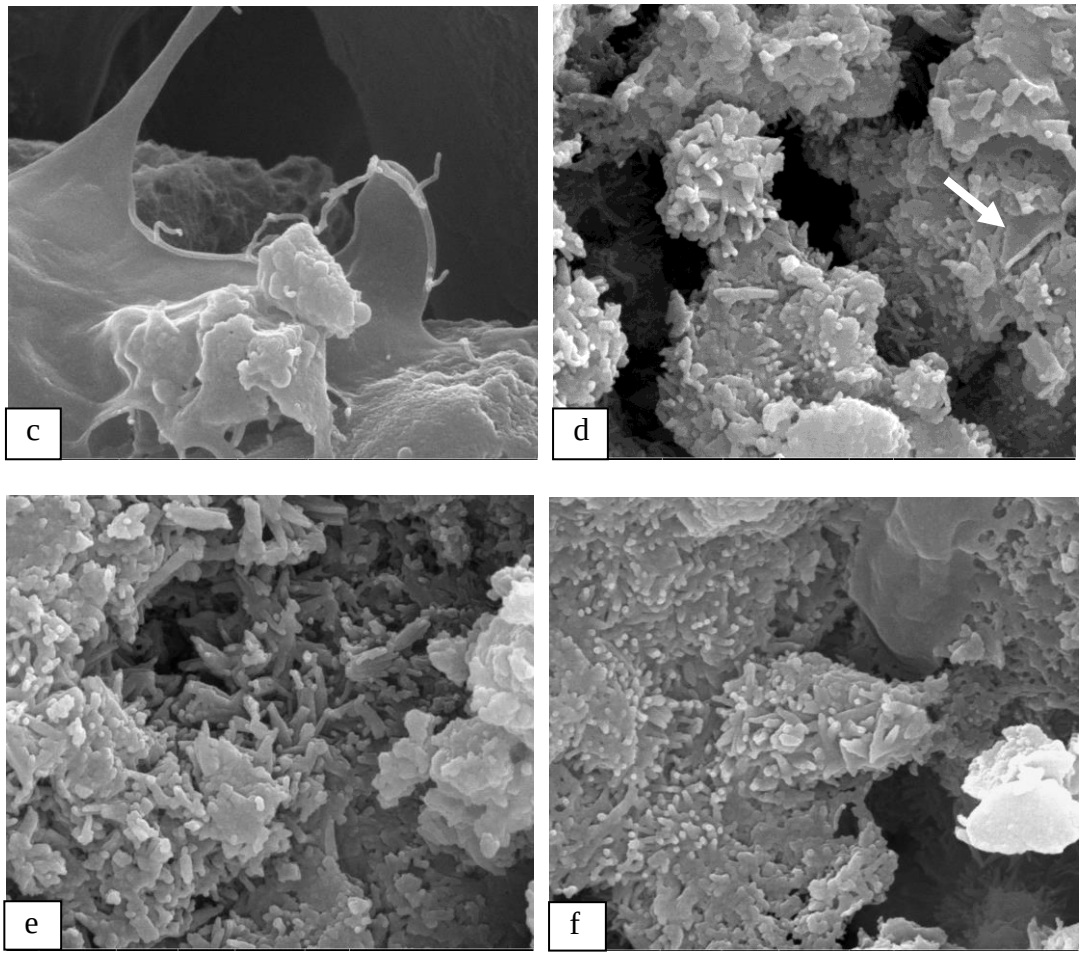

Figure 5. SEM of the CaP/chitosan/graphene coating soaked in the m-SBF for different periods (a) 0 week (b) 1 week (c) 4 weeks (d) 8 weeks (e) 10 weeks (f) 12 weeks

As the immersion time extended, the graphene could induce the deposition of phosphate on the coating and the graphene was gradually covered by the phosphate in Fig.5(d). When the immersion time reached to the 10 weeks and 12 weeks in Fig.5(e)(f), the lamellar structure of graphene was totally covered by the new phosphate.

3.2 Degradation behavior of Mg based CaP/chitosan/graphene in m-SBF

3.2.1 Electrochemical impedance

Table 1. Fitting results of Nyquist plots for Mg based CaP/chitosan/graphene soaked in m-SBF for different intervals

Time	1 Week	3 Weeks	4 Weeks	6 Weeks
R_{ct} /Ω·cm^2	46.96	54.94	628.9	530.2
R_s / Ω·cm^2	1403	440.5	898.4	
χ^2	5.9×10^{-4}	1.60×10^{-3}	2.80×10^{-3}	4.72×10^{-4}

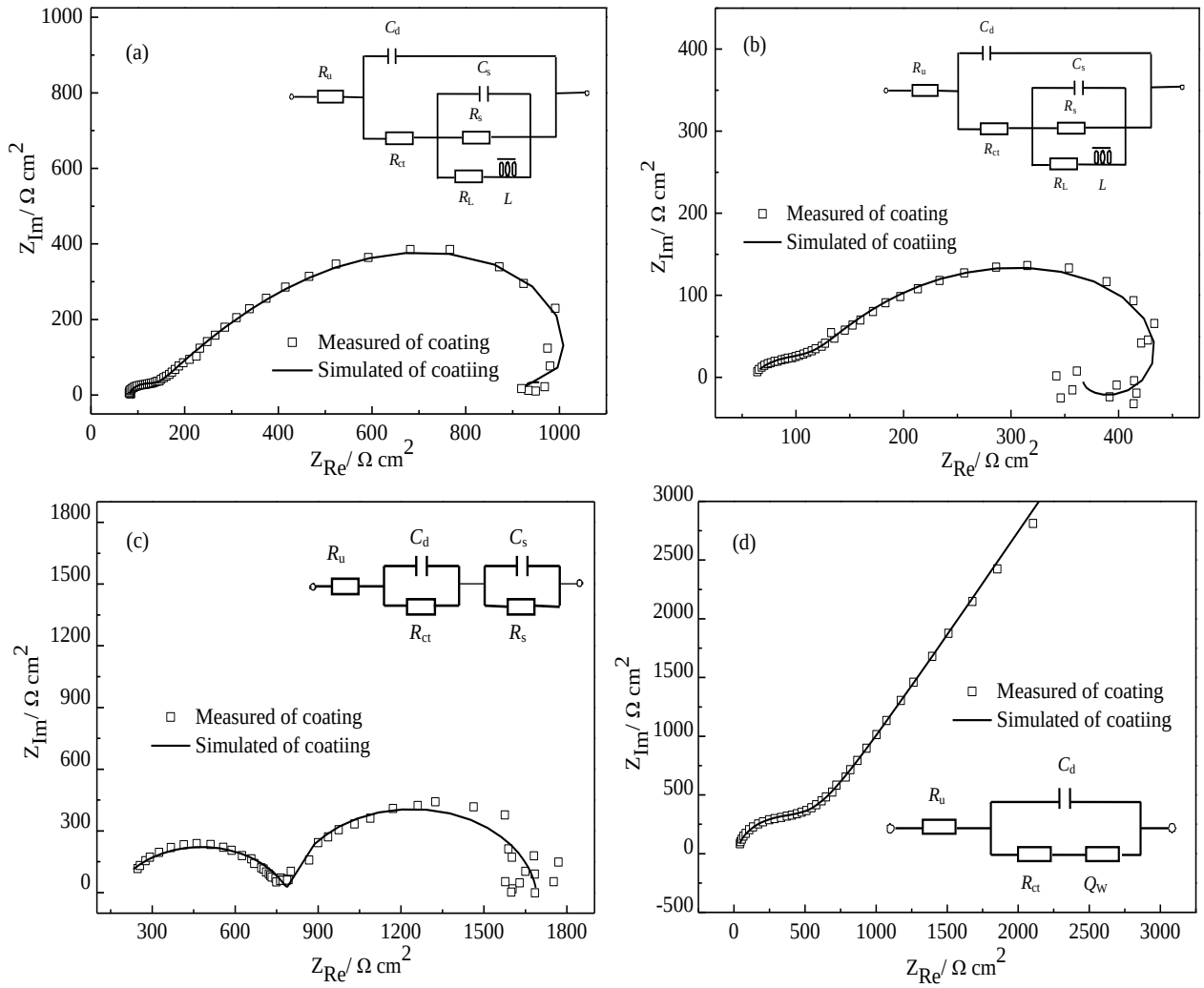

Figure 6. Nyquist plots and equivalent circuits of Mg based CaP/chitosan/graphene soaked in m-SBF for different intervals (a) 1 week; (b) 3 weeks; (c) 4 weeks; (d) 6 weeks

Figure 6 is Nyquist plots and the equivalent circuit of Mg based CaP/chitosan/ graphene in m-SBF for different intervals. Nyquist plots for different intervals was fitted according to the corresponding equivalent circuits, the fitting results are shown in Table1. Nyquist plots in Figure 6(a)(b)(c) are similar, they are composed of two capacitive reactance loops at the high-middle frequency region and a inductive impedance loop at low frequency region. Like the previous study[27], the capacitive reactance loop at high frequency area indicated the charge transfer resistance (R_{ct}) and double-electric layer capacitance (C_d) at interface, the capacitive reactance loop at middle frequency area corresponded to the resistance and capacitance of electrolyte through the corrosion product, MAO film and CaP/chitosan/graphene coating on the surface of Mg alloy, and the inductive impedance loop at low frequency area showed the adsorption and falling of the corrosion products on the interface between the solution and metal substrate[28-31].

In Figure 6 (d), Nyquist plot of sample was composed of a capacitive reactance loop at high frequency area and a oblique line at the middle-low frequency area. Moreover, the capacitive reactance loop at high frequency area was also charge transfer process, and a oblique line at the middle-low frequency was caused by a semi-infinite diffusion process.

When the Mg based CaP/chitosan/graphene was soaked in m-SBF for 1 week, 3 weeks and 4 weeks, it can be seen from Table 1 that R_{ct} increased and R_s showed a rough decreasing tendency. This was because the m-SBF permeated the coating in contact with the metal matrix and reacted with Mg alloys, the generated corrosion products on the interface between MAO-AZ91D Mg alloy and the coating caused the electrochemical reaction to occur difficultly. At the same time, the MAO layer was corroded by electrolyte, the calcium phosphate in the composite coating not only existed the deposition process but also the dissolving process. As a result, the above-mentioned comprehensive results resulted in the increase of R_{ct} and the decrease of R_f. When the soaking time was 6 weeks, the corrosion products on the metal substrate, MAO layer and the composite coating were all locally damaged, which would lead to the lack of protective layer of metal matrix, and the R_s reduced to zero (Table1), the corrosion behavior of the sample was controlled by the mixture process of electrochemistry and semi-infinite diffusion.

In conclusion, with the increase of soaking time in m-SBF, the corrosion behavior of Mg based CaP/chitosan/graphene was similar with Mg based CaP/chitosan in previous study[27]. In addition, in comparison with Mg based CaP/chitosan, the CaP/chitosan/graphene coating on Mg alloy was not destroyed when the immersion time in m-SBF was about 4 weeks(Fig.6(c)), which showed that the bonding between the coating and metal substrate was improved after addition graphene into CaP/chitosan coating.

3.2.2 Tafel curves

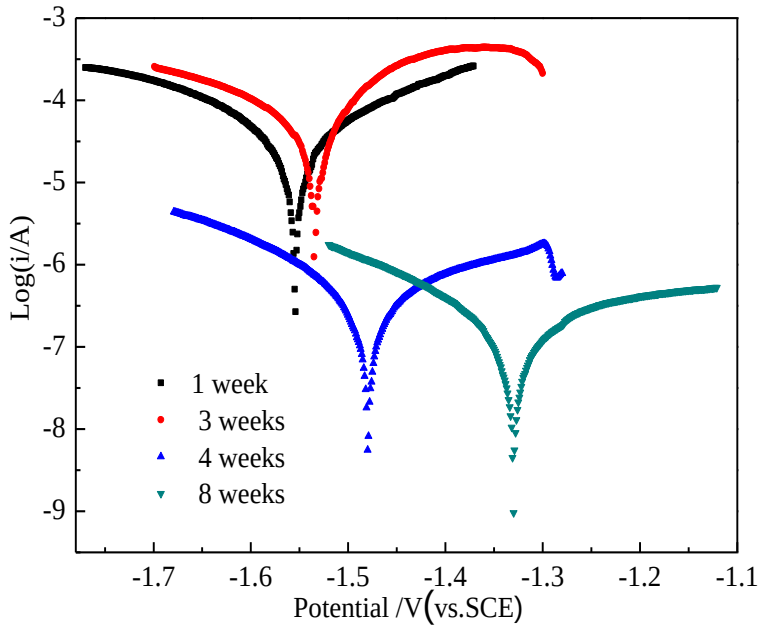

Figure 7. Tafel plots of Mg based CaP /chitosan/graphene soaked in m-SBF for different intervals

Tafel curves and the corresponding analysis results for Mg based CaP/chitosan/graphene soaked in m-SBF at different intervals are shown in Figure 7 and Table 2. It can be seen from Figure 7 and Table 2 that the i_{corr} value of Mg based CaP/chitosan/graphene showed a rough decrease trend

when the soaking time increased from 1 week to 8 weeks. Specifically, the coating was intact and i_{corr} value changed little from 1 weeks to 4 weeks, which indicated that the protective film made the electrochemical corrosion rate of samples be relatively stable. When the immersion time was greater than 4 weeks, the partial rupture of the coating and the direct contact between metal matrix and m-SBF caused the surface of Mg alloy to generate a dense layer of corrosion products, the i_{corr} value decreased instead[27].

Table 2. Results of Tafel plots for Mg based CaP/chitosan/graphene soaked in m-SBF for different intervals

Time	1 Week	3 Weeks	4 Weeks	8 Weeks
E_{corr}/V(vs·SCE)	-1.554	-1.534	-1.48	-1.330
i_{corr} /A·cm^{-2}	3.8×10^{-5}	7.7×10^{-5}	5.0×10^{-7}	1.9×10^{-7}

3.2.3 Immersion test

Figure 8 is the change of Mg element concentration and pH value in m-SBF as the soaking time for Mg based CaP/chitosan/graphene soaked in m-SBF. Figure 8(a)(b) showed that Mg element concentration and pH value in the whole soaking period increased, indicating that CaP/chitosan/graphene coating could not prevent Mg alloy from corroding in m-SBF and just decreased the corrosion rate of Mg alloy, as a result, Mg alloy in the m-SBF would slowly be degraded[18,32].

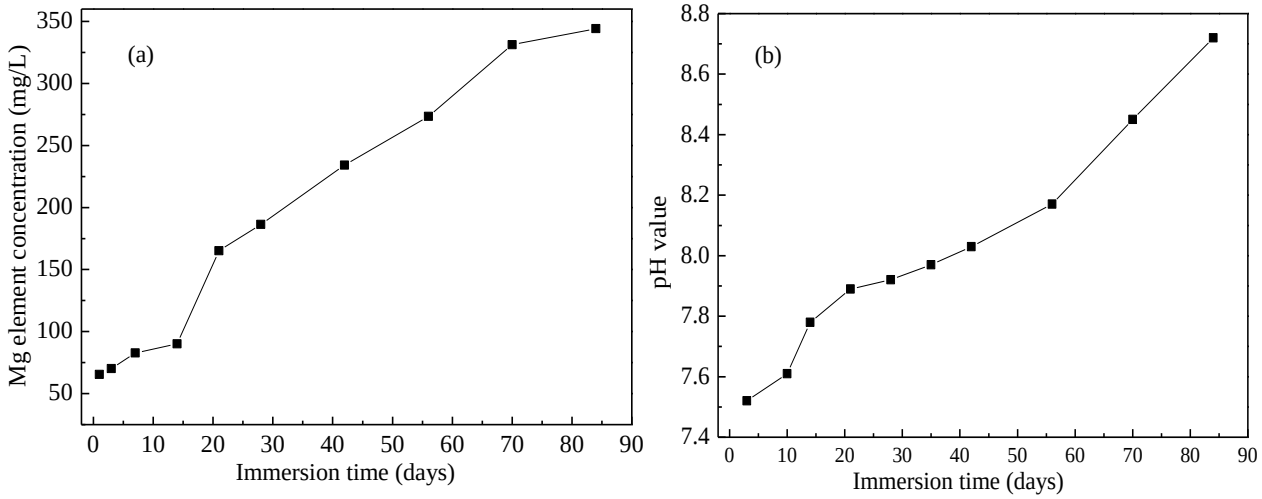

Figure 8. Changes of Mg concentration (a) and pH value (a) in m-SBF with the immersion time for Mg based CaP/chitosan/graphene

3.3 Cell viability test of the extracts from the immersion test

Fig.9 shows the SaOS-2 human cell viability that grew in the extracts from the soaking test. The extracts of Mg based CaP/chitosan/graphene were well tolerated by the osteoblasts with the cell

viability ranging from 123% to 103% until 16 days, which suggested that Mg based CaP/chitosan/graphene could not lead to the cell toxicity.

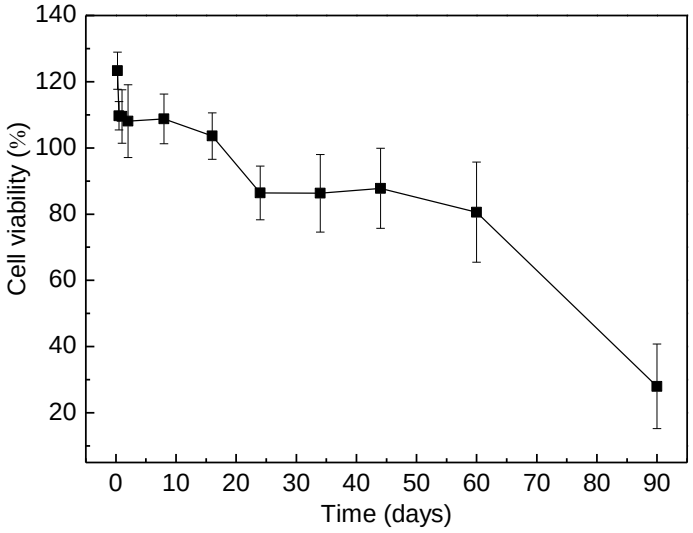

Figure 9. Cell viability of Mg based CaP/chitosan/graphene over time as derived from the absorbance reading at 450nm wavelength using the CCK assay

The cell viability of sample decreased as the immersion time further increased from 24 to 60 days, the cell viability was above 80% during this phase. The released amount of Mg^{2+} from Mg alloy and a rising pH value gradually increased as the increase of soaking time, which was connected with a decrease of cell viability. In this study, because the m-SBF in the soaking experiment was static, the concentration of Mg^{2+} and pH value were high in comparison with that in vivo environment. As a result, the cell viability was 28% when the soaking time reached to 90 days. Moreover, the cell viability of Mg based CaP/chitosan/graphene was higher than that of Mg based CaP/chitosan in previous study[32], which indicated that the addition of graphene contributed to improve the cell compatibility of Mg based CaP/chitosan.

4. CONCLUSIONS

In this paper, the CaP/chitosan/graphene coating has been successfully deposited on the Mg alloy. After Mg based CaP/chitosan/graphene was soaked in m-SBF, the negative charge on graphene could cause coating surface to form a layer of calcium enrichment film, which was conducive to the growth of phosphate. With the increase of immersion time, the bone-like apatite in CaP/chitosan/graphene coating gradually mineralized, while HA dissolved and then deposited. The corrosion reactions of Mg based CaP/chitosan/graphene in m-SBF was orderly controlled by electrochemical and finite-layer diffusion process, electrochemistry and semi-infinite diffusion process and semi-infinite diffusion process with the increase of soaking time. The cell viability of Mg based CaP/chitosan/graphene was satisfactory, the cell viability was above 80% within 60 days of immersion time.

ACKNOWLEDGEMENTS
This work was supported by the Natural Science Foundation of China (No. 81601616, No. 51671096), Science foundation of Heilongjiang province(No. H2016086), Postdoctoral fund in Heilongjiang province(LBH-Z15164) and Science and Technology Research Projects of Jiamusi University (No.12Z1201514)

References

1. A. L. Feng, Y. Han, *Materials and Dessign*, 32 (2011) 2813-2820.
2. F. E. Heakal, A. M. Fekry, M. Z. Fatayerji, *Journal of Appllied Electrochemistry*, 39(2009) 1633-1642.
3. J. Vormann, *Molecular Aspects Medicine*, 24(2003)27-37.
4. M. P. Staiger, A. M. Pietak, J. Huadmai, G. Dias, *Biomaterials*, 27(2006)1728-1734.
5. H. Hornberger, S. Virtanen, A. R. Boccaccini, *Acta Biomaterialia*, 8 (2012) 2442-2455.
6. S. A. Salman, K. Kuroda, M. Okido, *Bioinorganic Chemistry and Applications*, http://dx.doi.org/10.1155/2013/175756.
7. K. F. Bai, Y. Zhang, Z. Y. Fu , C. L. Zhang, X. Z. Cui, E. C. Meng , S. K. Guan, J. H. Hu, *Materials Letters*, 73(2012)59-61.
8. A. Biswas, I. S. Bayer, H. Zhao, T. Wang, F. Watanabe, A. S. Biris, *Biomacromolecules*, 11(2010) 2545-2549.
9. D. Lahiri, S. Ghosh, A. Agarwal, *Materials Science and Engineering C*, 32 (2012) 1727-1758.
10. M. Kalbacova, A. Broz, J. Kong, M. Kalbac, *Carbon*, 48(2010)4323-4329.
11. L. Zhang, W. W. Liu, C. G. Yue, T. H. Zhang, P. Li, Z. W. Xing, Y. Chen, *Carbon*, 61(2013) 105-115.
12. M. A. Rafiee, J. Rafiee, I. Srivastava, Z. Wang, H. H. Song, Z. Z. Yu, N. Koratkar, *Small*, 6(2010) 179-183.
13. R. Shepherd, S. Reader, A. Falshaw, *Glycoconjugate Journal*, 14(1997) 535-542.
14. A. Di Martino, M. Sittinger, M. V. Risbud, *Biomaterials*, 26 (2005) 5983-5990.
15. C. Durucan, P. W. Brown, *Advaned Engineering Materials*, 4(2001)227-231.
16. J. Zhang, C. S. Dai, J. Wei, Z. H. Wen, *Applied Surface Science*, 261(2012) 276-286.
17. J. Zhang, C. S. Dai, J. Wei, Z. H. Wen, S. J. Zhang, L. M. Lin, *Applied Surface Science* 280 (2013) 256– 262.
18. J. Zhang, C. S. Dai, J. Wei, Z. H. Wen, S. J. Zhang, C Chen, *Colloids and Surfaces B: Biointerfaces*, 11 (2013) 179–187.
19. C. J. Wu, Z. H. Wen, C. S. Dai, Y. X. Lu, F. X. Yang, *Surf. Coat. Technol.*, 204 (2010) 3336-3347.
20. T. Kokubo, H. Takadama, *Biomaterials*, 27 (2006) 2907-2915.
21. A. Oyane, H. M. Kim, T. Furuya, T. Kokubo, T. Miyazaki, T. Nakamura, *Journal of Biomedcial Materials Research A*, (2003) 188–195.
22. Q. G. Tan, K. Zhang, S. Y. Gu, J. Ren, *Applied Surface Science*, 255 (2009) 7036-7039.
23. J. Beuvelot, C. Bergeret, R. Mallet, V. Fernandez, J. Cousseau, M. F. Baslé, D. Chappard, *Acta Biomaterialia*, 6 (2010) 4110-4117.
24. G. M. Neelgund, A. Oki, Z. P. Luo, *Materials Research Bulletin*, 48 (2013) 175-179.
25. E. M. Duraia, A. Hannora, Z. Mansurov, G. W. Beall, *Materials Chemistry Physics*, 132 (2012)119-124.
26. G. Wei, J. T. Zhang, L. Xie, K. D. Jandt, *Carbon*, 49(2011)2216-2226.
27. J. Zhang, C. S. Dai, Z. H. Wen, J. Wei, *Int. J. Electrochem. Sci.*, 10 (2015) 6002-6013
28. M. Anik, G. Celikten, *Corrosion Science*, 49(2007) 1878-1894
29. J. W. Chang, X. W. Guo, S. M. He, P. H. Fu, L. M. Peng, W. J. Ding, *Corrosion Science*, 50(2008)166-177

30. M. Anik, G. Celikten, *Corrosion Science*, 49(2007) 1878-1894
31. M. Jamesh, S. Kumar, T. S. N. Sankara Narayanan, *Corrosion Science*, 53 (2011) 645-654
32. J. Zhang, Z. H. Wen, M. Zhao, G. Z. Li, C. S. Dai, *Materials Science and Engineering C*, 58 (2016) 992–1000